

# Dynamic Susceptibility MR Perfusion in Diagnosing Recurrent Brain Metastases After Radiotherapy: A Systematic Review and Meta-Analysis

Robert M. Kwee, MD, PhD,<sup>1</sup>  and Thomas C. Kwee, MD, PhD<sup>2\*</sup>

**Background:** The diagnostic performance of dynamic susceptibility contrast (DSC) MR perfusion in discriminating treatment-related changes from recurrence in irradiated brain metastases is currently not completely clear.

**Purpose:** To systematically review the accuracy of DSC MR perfusion in diagnosing recurrent brain metastases after radiotherapy.

**Study Type:** Systematic review and meta-analysis.

**Subjects:** MEDLINE and Embase were searched for original studies investigating the accuracy of DSC MR perfusion in diagnosing recurrent brain metastases after radiotherapy. Ten studies, comprising a total of more than 271 metastases, were included.

**Field Strength/Sequence:** 1.5T or 3.0T, DSC MR perfusion.

**Assessment:** Quality assessment was performed according to the Quality Assessment of Diagnostic Accuracy Studies-2 tool.

**Statistical Tests:** Sensitivity and specificity were pooled with a bivariate random-effects model. Heterogeneity was assessed by a chi-squared test. Potential sources for heterogeneity were explored by subgroup analyses.

**Results:** In seven studies the diagnostic criterion was not prespecified. In eight studies it was unclear whether the reference standard was interpreted blindly. In seven studies it was unclear whether DSC MR perfusion results influenced which reference standard was used. Pooled sensitivity and specificity were 81.6% (95% confidence interval [CI]: 70.6%, 89.1%) and 80.6% (95% CI: 64.2%, 90.6%), respectively. There was significant heterogeneity in both sensitivity ( $P = 0.005$ ) and specificity ( $P < 0.001$ ). There were no significant differences in relative diagnostic odds ratio according to publication year, country of origin, study size, and DSC MR perfusion interpretation method (visual analysis of cerebral blood volume [CBV] map vs. relative CBV measurement) ( $P > 0.2$ ). Due to insufficiently detailed reporting, it was not possible to investigate the influence of primary tumor origin on accuracy.

**Data Conclusion:** Our results suggest that the accuracy of DSC MR perfusion in diagnosing recurrent brain metastases after radiotherapy is fairly high. However, these findings should be interpreted with caution because of methodological quality concerns and heterogeneity between studies.

**Level of Evidence:** 3

**Technical Efficacy:** Stage 2

J. MAGN. RESON. IMAGING 2020;51:524–534.

**B**RAIN METASTASES are the most common malignant intracranial neoplasms in adults.<sup>1</sup> They occur in ~2% of all patients with newly diagnosed invasive solid cancer.<sup>2</sup> Because of increased surveillance and improved systemic control, the incidence is likely to grow.<sup>1</sup> Brain metastases are associated with significant morbidity and mortality.<sup>2</sup> Current

care involves stereotactic or whole-brain radiotherapy and/or surgery, depending on the number, size, and site of metastases, as well as overall systemic disease control and patient's performance status.<sup>1</sup>

An estimated one-third of brain metastases increase in size after irradiation and the longer the patient survives, the more likely

View this article online at [wileyonlinelibrary.com](http://wileyonlinelibrary.com). DOI: 10.1002/jmri.26812

Received Apr 17, 2019, Accepted for publication May 17, 2019.

\*Address reprint requests to: T.C.K., Department of Radiology, Nuclear Medicine and Molecular Imaging, University Medical Center Groningen, University of Groningen, Hanzeplein 1, P.O. Box 30.001, 9700 RB Groningen, The Netherlands. E-mail: [thomaskwee@gmail.com](mailto:thomaskwee@gmail.com)

From the <sup>1</sup>Department of Radiology, Zuyderland Medical Center, Heerlen/Sittard/Geleen, The Netherlands; and <sup>2</sup>Department of Radiology, Nuclear Medicine and Molecular Imaging, University Medical Center Groningen, Groningen, The Netherlands

This is an open access article under the terms of the Creative Commons Attribution-NonCommercial-NoDerivs License, which permits use and distribution in any medium, provided the original work is properly cited, the use is non-commercial and no modifications or adaptations are made.

an increase in lesion size will be seen on follow-up imaging.<sup>3</sup> This increase in size occurs secondary to blood–brain barrier disruption with accumulation of paramagnetic agents in the extracellular space and is nonspecific<sup>4,5</sup>: it can represent either treatment-related changes (pseudoprogression or radionecrosis) or metastatic recurrence. Because of the similar appearance, they are difficult to discriminate on conventional contrast-enhanced magnetic resonance imaging (MRI).<sup>4–6</sup> Accordingly, lesion measurements on conventional postgadolinium T<sub>1</sub>-weighted and T<sub>2</sub>-weighted images are not significantly associated with either treatment-related changes or metastatic recurrence.<sup>5</sup> One study suggested that the ratio of the lesion as seen on T<sub>2</sub>-weighted images to the total enhancing area on postgadolinium T<sub>1</sub>-weighted images could be useful,<sup>7</sup> but a later independent study found this so-called lesion quotient not to be discriminative, with sensitivity and specificity of only 59% and 41%, respectively.<sup>5</sup> However, early and accurate diagnosis is important, since patients with treatment-related changes can undergo watchful waiting, whereas patients with metastatic recurrence are potential candidates for surgery or repeated stereotactic radiotherapy.<sup>8,9</sup> Histopathologic confirmation is the current gold standard,<sup>5</sup> but biopsy/surgery is invasive, with potential complications such as hemorrhage and infection.<sup>10</sup> There is therefore a need for a noninvasive tool that can accurately diagnose recurrent brain metastases after radiotherapy. Dynamic susceptibility contrast (DSC) MR perfusion may be used to discriminate treatment-related changes from metastatic recurrence.<sup>11,12</sup> DSC MR perfusion uses the first-pass susceptibility effect of a gadolinium-based contrast agent within the intravascular compartment.<sup>11,12</sup> It allows assessment of several hemodynamic imaging variables. The relative cerebral blood volume (rCBV) is the most widely used hemodynamic variable derived from DSC MR perfusion and has been shown to correlate with primary glioma tumor grade and tumor microvascular density.<sup>11,12</sup> rCBV is generally elevated in viable or recurrent metastases after radiotherapy but not in treatment-related changes<sup>11,12</sup>

(Figs. 1–2). However, the diagnostic performance of DCS MR perfusion is currently not completely clear. Therefore, the purpose of this study was to systematically review the accuracy of DCS MR perfusion in diagnosing recurrent brain metastases after radiotherapy.

## Materials and Methods

### Data Sources

A search in MEDLINE and Embase was conducted to find publications on the accuracy of DSC MR perfusion in diagnosing recurrent brain metastases after radiotherapy. The following search terms were used: (brain OR cerebral OR intracranial) AND (metastases OR metastasis OR metastatic) AND (magnetic resonance OR MR imaging OR MRI OR magnetic resonance tomography OR nuclear magnetic resonance OR NMR) AND (perfusion OR dynamic OR susceptibility OR DSC). The search was updated until October 2018. Bibliographies of studies which finally remained after the selection process were screened for potentially suitable references.

### Study Selection

Original studies investigating the accuracy of DSC MR perfusion in diagnosing recurrent brain metastases after radiotherapy were eligible for inclusion. Studies involving  $\leq 10$  patients with brain metastases were excluded. Studies that only investigated the accuracy of dynamic contrast-enhanced MR perfusion (relying on T<sub>1</sub> shortening due to gadolinium-based contrast) or arterial spin labeling were excluded. Studies that only assessed change in DSC MR perfusion before and after radiotherapy as a predictor of tumor response were also excluded. Studies that provided insufficient data to construct a 2 × 2 contingency table to calculate sensitivity and specificity were also excluded. With the use of the aforementioned selection criteria, titles and abstracts of retrieved studies were reviewed. Full-text versions of potentially eligible articles were retrieved. Full-text articles were then reviewed to definitively determine if the study was eligible for inclusion.

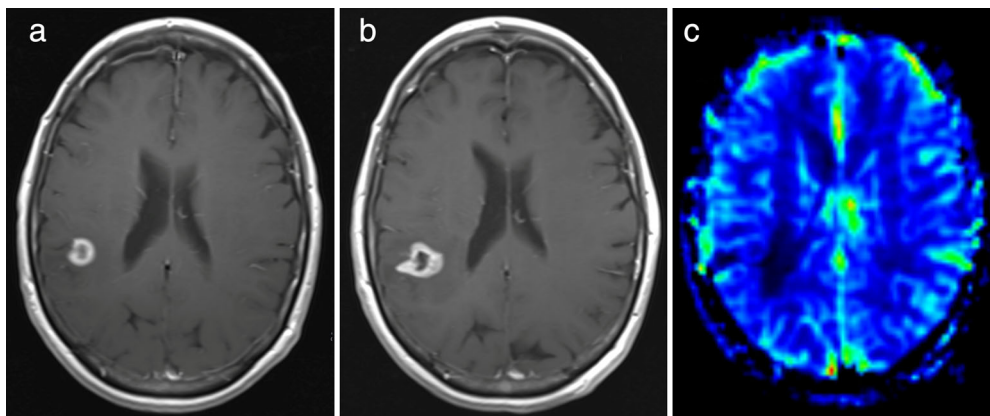


**FIGURE 1:** Pseudoprogression of brain metastasis from nonsmall-cell lung cancer in the right parietotemporal region in a 60-year-old woman. Axial contrast-enhanced T<sub>1</sub>-weighted image 6 months after stereotactic radiotherapy (b) shows increased size of the contrast-enhancing lesion compared with 3 months before (a). At the CBV map 6 months after stereotactic radiotherapy (c) no highly vascularized areas within the contrast-enhancing lesion are seen, indicative of pseudoprogression. Further follow-up showed decreasing size of the lesion (MR images not shown), confirming pseudoprogression.

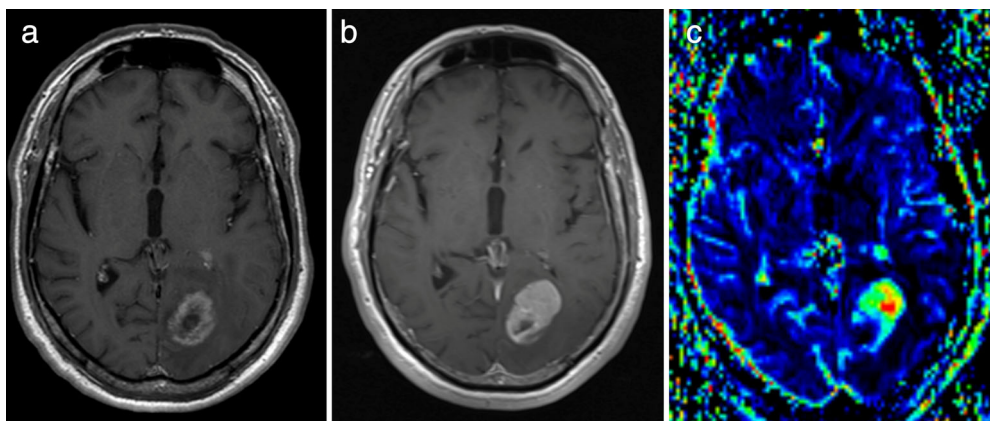


**FIGURE 2:** Recurrent metastasis originating from nonsmall-cell lung cancer in the left occipital lobe in a 69-year-old man. Axial contrast-enhanced T<sub>1</sub>-weighted image 6 months after stereotactic radiotherapy (b) shows increased size of the contrast-enhancing lesion compared with 3 months before (a). At the CBV map 6 months after stereotactic radiotherapy (c) highly vascularized areas within the contrast-enhancing lesion are seen, indicative of recurrence. The lesion was subsequently resected and histopathological analysis confirmed metastatic recurrence.

### Study Data Extraction

For each included study, principle characteristics (Table 1) and true positive, false positive, false negative, and true negative values of DSC MR perfusion in diagnosing recurrent brain metastases were extracted.

#### Study Quality Assessment

Study quality was assessed by using the Quality Assessment of Diagnostic Accuracy Studies 2 (QUADAS-2) tool, which comprises four key domains: "patient selection," "index test," "reference standard," and "flow and timing."<sup>13</sup>

### Statistical Analyses

Sensitivity and specificity of individual studies were calculated. A bivariate random-effects model was used for meta-analysis.<sup>9</sup> Individual studies were plotted in receiver operating characteristic (ROC) space, as were the summary estimate with 95% confidence ellipse.<sup>14</sup> A chi-squared test was performed to test for heterogeneity. Potential sources for heterogeneity were explored by assessing whether certain covariates significantly influenced the relative diagnostic odds ratio (RDOR).<sup>15</sup> Prespecified covariates were publication year (published before vs. in or after 2013 [2013 was the median]), country of origin (USA vs. other countries), study size (<28 vs. >28 patients [28 was the median]), and DSC MR perfusion interpretation method (visual analysis of CBV map vs. rCBV measurement). In studies that performed both visual analysis of CBV map and rCBV measurement, we compared the area under the ROC curve (AUC) for both methods.<sup>16</sup> Potential publication bias was assessed by a funnel plot.<sup>17</sup> Statistical analyses were performed using Meta-analysis of Diagnostic Accuracy Studies package in R software<sup>18,19</sup> and MedCalc Statistical Software, v. 15.8 (MedCalc Software, Ostend, Belgium).  $P < 0.05$  was considered statistically significant for all analyses.

## Results

### Literature Search

The study selection process is displayed in Fig. 3. Fifteen studies were potentially eligible for inclusion.<sup>8,11,20–32</sup> After reviewing the full text, one study was excluded because the accuracy of DSC MR perfusion was not investigated<sup>24</sup>; two studies were excluded because only a change in DSC MR perfusion before

and after radiotherapy as predictor of metastatic tumor response was assessed,<sup>31,32</sup> one study was excluded because it provided insufficient data for a  $2 \times 2$  contingency table,<sup>27</sup> and one study was excluded because no separable data on the accuracy of DSC MR perfusion were reported.<sup>25</sup> Eventually, 10 studies were included.<sup>8,11,20–23,26,28–30</sup>

The median number of patients per study was 28 (range 15–46). DSC MR perfusion data were available on 271 metastases. The median prevalence of recurrent brain metastases was 56.9% (range 7.7%–83.3%).

### Methodologic Quality Assessment

QUADAS-2 assessments are displayed in Table 2 and summarized in Fig. 4. Risk of bias with respect to patient selection was rated "unclear" in two studies<sup>5,28,30</sup> because it was unclear whether a consecutive or random sample was enrolled and whether there were no inappropriate exclusions. Risk of bias with respect to index test was rated "high" in seven studies<sup>11,20–22,26,28,29</sup> because diagnostic criteria were not prespecified. Risk of bias with respect to reference standard was rated "unclear" in eight studies,<sup>8,11,20,22,23,26,28,29</sup> because it was unclear whether the reference standard was interpreted without knowledge of the results of DSC MR perfusion. Risk of bias with respect to flow and timing was rated "unclear" in seven studies<sup>11,20,22,23,26,28,30</sup> because it was unclear whether DSC MR perfusion results influenced the decision which reference standard was used. Risk of bias with respect to flow and timing was rated "high" in one study,<sup>8</sup> because not all patients were included in the analysis. In two studies,<sup>22,23</sup> there were applicability concerns with respect to patient selection, because both stable and progressive metastases at conventional MR (contrast-enhanced T<sub>1</sub>-weighted MR images) were included. There were no other applicability concerns.

### Diagnostic Performance

Different diagnostic criteria were used (Table 1). Both sensitivity and specificity from individual studies ranged from 0%

**TABLE 1. Principal Study Characteristics**

Study	Publication year, country of origin	Number of patients, age and sex	Primary tumors (%)	DSC MR perfusion parameters- Field strength- Pulse sequence- TR, TE, flip angle- Slice thickness- FOV, matrix- Temporal coverage- Gd preload- Gd dose- Injection rate	Image processing tools	Observers	Diagnostic criteria for recurrence	Uninterpretable lesions (%)	Reference standard (%) <sup>a</sup>	Prevalence of recurrent brain metastases (%)
Wang et al <sup>20</sup>	2018, China	46, median age 61 years (range 30-80), 22 males	Lung (56.9) Breast (17.2) Skin (8.6) Renal (8.6) Colon (8.6)	- 3 T - GRE-EPI - 1600, 30, 90° - 4 mm - 220 × 220, 120 × 120 - 50 measurements - NR - 0.2 mmol/kg - 4.5 ml/s	Commercially available software (Syngo.via; Siemens Healthcare)	Two neuroradiologists (both with over 15 years of experience)	- CBV lesion >21.8 ml/100g - rCBV (mean CBV lesion/mean CBV NACWM) >2.12	8.8	Histopathology (9%) <sup>b</sup> or MRI + clinical follow-up (91%)	56.9
Knitter et al <sup>21</sup>	2018, USA	29, median age 56 years (interquartile range 48-64.5), 10 males	Lung (40.6) Breast (31.3) Melanoma (9.4) Renal (6.3) Neuroendocrine tumor (3.1)	- 1.5 T or 3T - GRE-EPI - 1800, 40, 90° - 5 mm - 220 × 220, 128 × 128 - 60 measurements - Yes - 0.1 mmol/kg - 5 ml/s	Commercially available (Olea Sphere, Olea Medical)	NR	rCBV (mean CBV lesion/mean CBV NACWM) >2.1	0	MRI follow-up (100%)	31.3
Muto et al <sup>22</sup>	2018, Italy	29 (mean age 53 years (range 33-79), 11 males)	Breast (44.8) Lung (41.4) Bladder (6.9) Colon (6.9)	- 1.5 T - GRE-EPI - NR - NR - NR - NR - 0.1 mmol/kg - 4.5 ml/s	Commercially available (Olea Sphere, Olea Medical)	Two neuroradiologists with 4 and 5 years of experience	rCBV (CBV lesion <sup>a</sup> / NACWM <sup>a</sup> ) >2.1	0	Histopathology (NR) <sup>b</sup> or MRI + clinical follow-up (NR)	32.1
Kerkhof et al <sup>23</sup>	2018, The Netherlands	26, median age 66 years (range 40-84), 12 males	NSCLC (46.2) Breast cancer (19.2) Other (34.6)	- 1.5 T - GRE-EPI - 1490, 30, 90° - 5 mm - 230 × 230, 128 × 128 - NR - Yes - 20 ml Gd - 4 ml/s	Not reported	Two experienced neuroradiologists	Visually highly vascularized areas within the contrast-enhancing lesion relative to the contralateral hemisphere	15.5	Histopathology <sup>c</sup> (NR) or MRI follow-up (NR)	7.7

TABLE 1. Continued

Study	Publication year, country of origin	Number of patients, age and sex	Primary tumors (%)	DSC MR perfusion parameters- Field strength- Pulse sequence- TR, TE, flip angle- Slice thickness- FOV, matrix- Temporal coverage- Gd pre-load- Gd dose- Injection rate	Image processing tools	Observers	Diagnostic criteria for recurrence	Uninterpretable lesions (%)	Reference standard (%) <sup>a</sup>	Prevalence of recurrent brain metastases (%)
Cicone et al <sup>26</sup>	2015, Italy	42, median age 64 years (range 38-84), NR	NSCLC (42.0) Breast (14.0) Renal (10.0) Colon (8.0) Melanoma (8.0) SCLC (6.0) Bladder (4.0) Thyroid (4.0) Gastric (2.0) Cervical (2.0)	- 1.5 T - GRE-EPI - 1490, 40, 90° - 5 mm - 230 × 230, 128 × 128 - 50 measurements in 78 s - Yes - 0.1 mmol/kg - 4 ml/s	Commercially available workstation (Leonardo, Siemens Healthcare)	Two experienced readers in consensus	rCBV (maximum) CBV lesion/mean CBV NACWM(> 2.14	7.1	Histopathology <sup>d</sup> (22%) or MRI follow-up (78%)	40.5
Huang et al <sup>28</sup>	2011, USA	26, NR, NR	Lung (51.5) Breast (33.3) Esophagus (6.1) Melanoma (6.1) Renal (3.0)	- 1.5 T - GRE-EPI - 2480, 98, NR - 4 mm - NR (voxel size: 2 × 2 × 4) - 50 measurements in 125 s - NR - 0.1 mmol/kg - 3 ml/s	Commercially available workstation (Pinnacle)	Experienced, board-certified neuroradiologists	rCBV (maximum) CBV lesion/maximum CBV NACWM(> 2	3.6	Histopathology <sup>e</sup> (12%) or MRI + clinical follow-up (88%)	66.7
Mitsuya et al <sup>29</sup>	2010, Japan	27, mean age 59.5 years (range 38-85), 14 males	Lung (53.6) Breast (32.1) Colon (7.1) Esophagus (7.1)	- 1.5 T - SE-EPI - 500, 33, 90° - 6 mm - 220 × 220, 128 × 128 - NR - Yes - 0.1 mmol/kg - 5 ml/s	Commercially available (Philips Easy Vision, Philips Healthcare)	An observer	rCBV (CBV lesion/ CBV NACWM <sup>a</sup> ) >2.1	0	MRI + clinical follow-up (100%)	25.0
Hoeftagels et al <sup>30</sup>	2009, The Netherlands	31, mean age 54.0 years (range 36-72), 12 males	Lung (58.8) Breast (14.7) Ovary (8.8) Melanoma (5.9) Renal (5.9) Bladder (2.9) Colon (2.9)	- 1.5 T - GRE-EPI - 1440, 47, 90° - 5 mm - 230 × 230, 128 × 128 - 50 measurements in 72 s - NR - 0.1 mmol/kg - 5 ml/s	Commercially available (Leonardo, Siemens Healthcare)	An experienced neuroradiologist	- Presence of nodular highly vascularized areas within the contrast-enhancing lesion - rCBV (maximum CBV lesion/mean CBV NACWM) >2.0 - rCBV (maximum CBV lesion/mean CBV NACGM) >1.85	0	Histopathology <sup>e</sup> (18%) or MRI + clinical follow-up (82%)	20/34

TABLE 1. Continued

Study	Publication year, country of origin	Number of patients, age and sex	Primary tumors (%)	DSC MR perfusion parameters- Field strength- Pulse sequence- TR, TE, flip angle- Slice thickness- FOV, matrix- Temporal coverage- Gd pre-load- Gd dose- Injection rate	Image processing tools	Observers	Diagnostic criteria for recurrence	Uninterpretable lesions (%)	Reference standard (%) <sup>a</sup>	Prevalence of recurrent brain metastases (%)
Barajas et al. <sup>11</sup>	2009, USA	27, NR, 11 males	Lung (59.3) Breast (29.6) Renal (7.4) Extremity sarcoma (3.7)	- 1.5 T - GRE-EPI - 1000-1250, 54, 35° - NR - NR - 60 measurements in 75 s - NR - 0.1 mmol/kg - 4 or 5 ml/s	Commercially available (Advantage Workstation, GE Healthcare).	An attending neuroradiologist	rCBV (CBV lesion/ <sup>7</sup> NACWM <sup>8</sup> ) >1.52	16.7	Histopathology <sup>5</sup> (73%) or MRI + clinical follow-up (27%)	58.8
Truong et al. <sup>8</sup>	2006, USA	15, NR, NR	NR	- NR - SE-EPI - 100, 54, 90° - 5 or 7 mm - 230 × 230, 128 × 128 - 60 measurements - 0.1 mmol/kg - NR - 5 ml/s	Commercially available (Unix workstation) using in-house software	NR	rCBV (maximum CBV lesion/mean CBV NACWM) >1.52	20.0	Histopathology <sup>5</sup> (100%)	83.3

GRE-EPI: gradient echo echo-planar imaging; NACWM: normal-appearing contralateral white matter; NACGM: normal-appearing contralateral gray matter; NR: not reported; rCBV: relative cerebral blood volume; SE-EPI: spin echo echo-planar imaging

<sup>a</sup>Percentage of lesions that were verified by this reference standard.

<sup>b</sup>Not further specified.

<sup>c</sup>Presence of viable tumor.

<sup>4</sup>≥20% neoplastic features in the surgical specimen.

<sup>5</sup>>1% viable tumor.



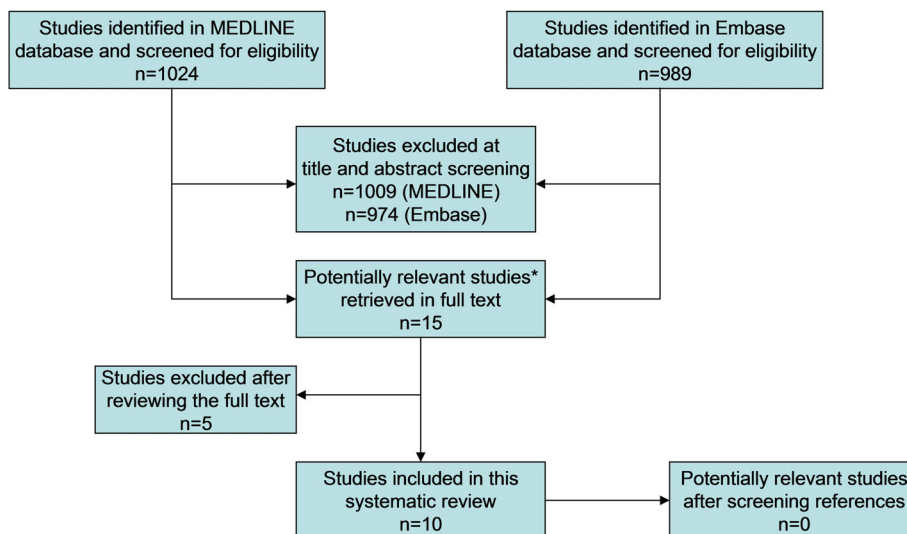


FIGURE 3: Flowchart of the study selection process. \*All 15 potentially relevant studies were found in both databases.

to 100% (Fig. 5), with pooled estimates of 81.6% (95% confidence interval [CI]: 70.6%, 89.1%) and 80.6% (95% CI: 64.2%, 90.6%), respectively. The ROC plot is shown in Fig. 6. The AUC was 0.873. All studies, except Muto et al’s study,<sup>22</sup> reported accuracy data on a per-lesion basis. Muto et al’s study<sup>22</sup> used number of MR examinations (mean of 2.69 per patient) for accuracy analysis. Excluding this study<sup>22</sup> from meta-analysis resulted in pooled sensitivity of 79.4% (95% CI: 68.6%, 87.2%) and pooled specificity of 77.3% (95% CI: 61.6%, 87.9%), with an AUC of 0.847.

The median percentage of uninterpretable lesions per study was 5.35 (range 0–20.0) (Table 1). In one study,<sup>30</sup> six

lesions were excluded from accuracy analysis because visual CBV map analysis was nonconclusive.

The included studies were heterogeneous in sensitivity ( $P = 0.005$ ) and specificity ( $P < 0.001$ ). RDORs were not significantly different in subgroups according to publication year, country of origin, study size, and DSC MR perfusion interpretation method (Table 3). In the only included study that performed both visual analysis of the CBV map and rCBV measurement,<sup>30</sup> AUCs did not significantly differ: AUC of 0.813 (95% CI: 0.621, 0.934) for visual analysis of CBV map vs. AUC of 0.754 (95% CI, 0.556, 0.896) for rCBV measurement ( $P = 0.6167$ ).

TABLE 2. QUADAS-2 Assessment Results of Each of the Included Studies

Study	Risk of bias				Applicability concerns		
	Patient selection	Index test	Reference standard	Flow and timing	Patient selection	Index test	Reference standard
Wang et al <sup>20</sup>	Low	High	Unclear	Unclear	Low	Low	Low
Knitter et al <sup>21</sup>	Low	High	Low	Low	Low	Low	Low
Muto et al <sup>22</sup>	Low	High	Unclear	Unclear	High	Low	Low
Kerkhof al. <sup>23</sup>	Low	Unclear	Unclear	Unclear	High	Low	Low
Cicone et al <sup>26</sup>	Low	High	Unclear	Unclear	Low	Low	Low
Huang et al <sup>28</sup>	Low	High	Unclear	Unclear	Low	Low	Low
Mitsuya et al <sup>29</sup>	Low	High	Unclear	Low	Low	Low	Low
Hoefnagels et al <sup>30</sup>	Unclear	Low	Low	Unclear	Low	Low	Low
Barajas et al <sup>11</sup>	Low	High	Unclear	Unclear	Low	Low	Low
Truong et al <sup>8</sup>	Unclear	Unclear	Unclear	High	Low	Low	Low

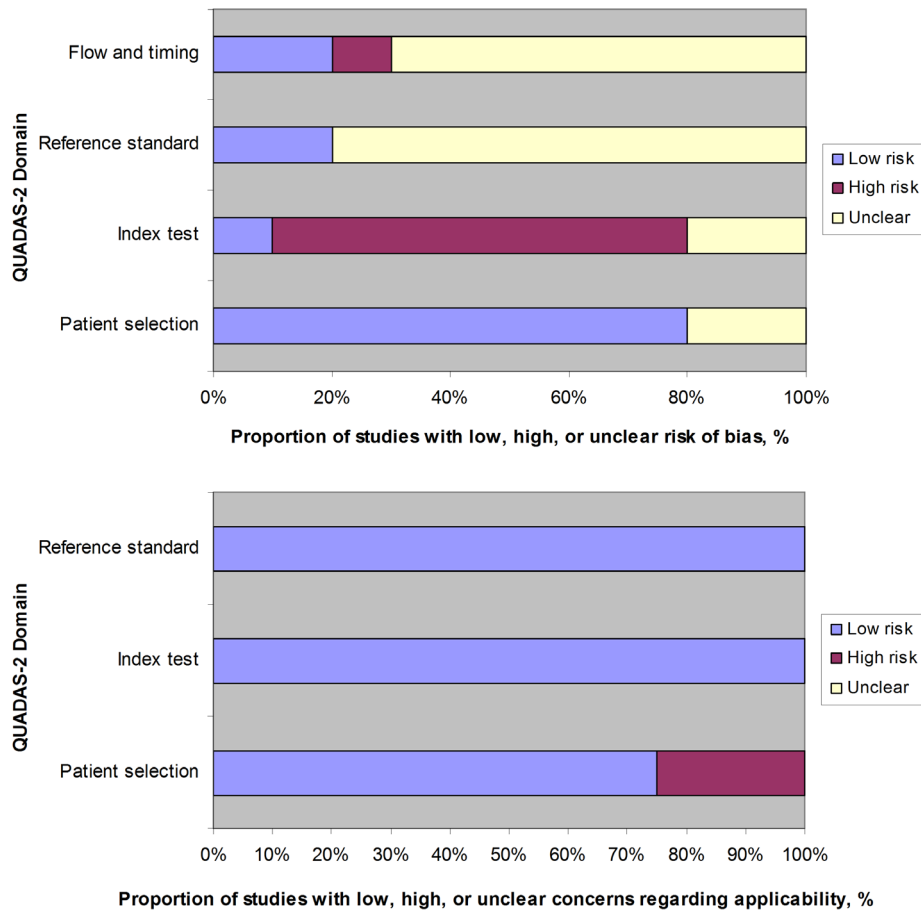


FIGURE 4: Summary of QUADAS-2 assessments of the 10 included studies.

The funnel plot (Fig. 7) was roughly symmetrical, suggesting a low likelihood of publication bias.

### Discussion

This systematic review investigated the accuracy of DSC MR perfusion in diagnosing recurrent brain metastases after radiotherapy. Different diagnostic criteria were used by the included studies to define metastatic recurrence. We used a bivariate random-effects

model for meta-analysis, which acknowledges a possible threshold effect.<sup>14</sup> Pooled sensitivity and specificity were fairly high, but there was significant between-study heterogeneity.

Potential bias in the domains "index test," "reference standard," and "flow and timing" may have resulted in overestimation of accuracy. In clinical practice, DSC MR perfusion is typically used to differentiate treatment-related changes from recurrence in irradiated metastases which show a new area of enhancement and/or enlargement at conventional MR. There

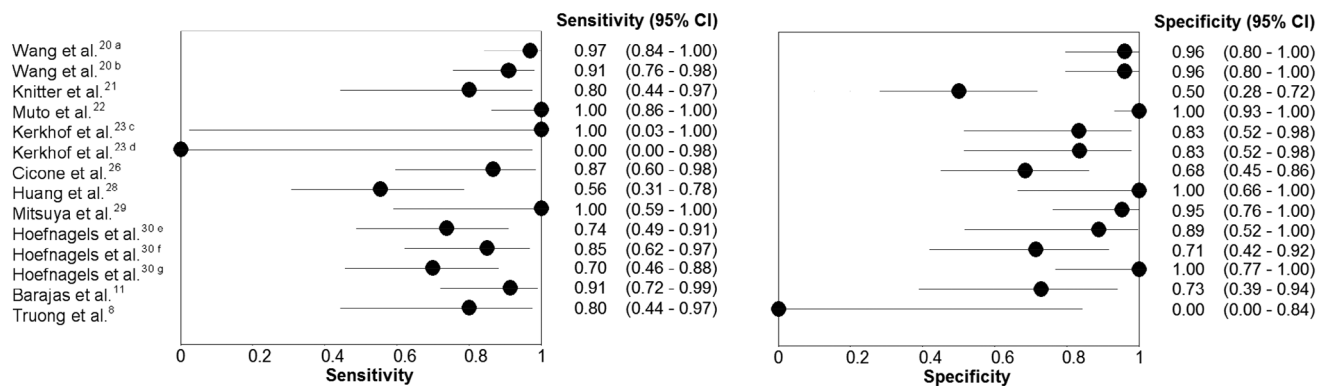
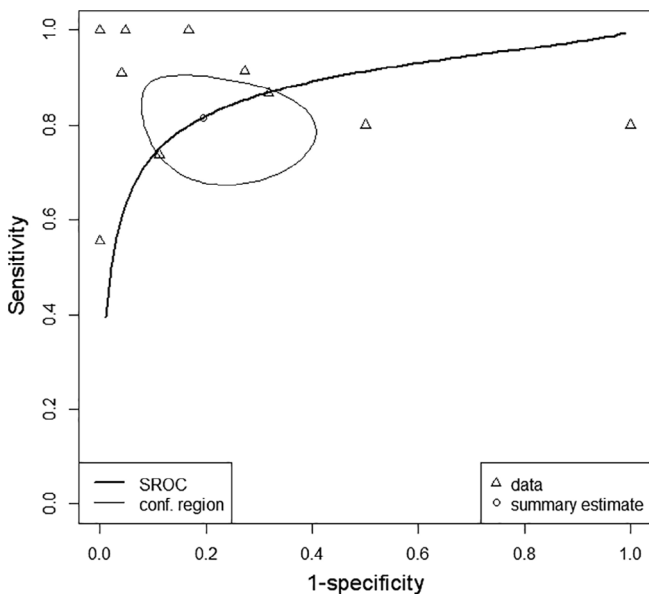


FIGURE 5: Forest plots of sensitivity and specificity of included studies. <sup>a</sup>absolute CBV; <sup>b</sup>rCBV; <sup>c</sup>At 3 months follow-up; <sup>d</sup>At 6 months follow-up; <sup>e</sup>Subjective scoring of CBV map; <sup>f</sup>rCBV (maximum CBV lesion/mean CBV NACWM); <sup>g</sup>rCBV (maximum CBV lesion/mean CBV NACGM).





**FIGURE 6:** Receiver operating characteristic plot. \*Individual study data (small triangles) have been plotted in ROC space, as were the summary estimate (small circle) with 95% confidence ellipse (oval area, thin line) and summary receiver operating characteristic curve (thick line). \*From Wang et al’s study,<sup>20</sup> rCBV data were used; from Kerkhof et al’s study,<sup>23</sup> 3-month follow-up data were used; and from Hoefnagels et al’s study,<sup>30</sup> data from visual CBV map analysis were used for analysis. SROC: summary receiver operating characteristic curve; conf. region: 95% confidence ellipse of pooled sensitivity and specificity.

were applicability concerns with respect to patient selection in two studies,<sup>22,23</sup> because they included both stable and progressive metastases at conventional MR. However, DSC MR perfusion may also have value in metastases that show stability or regression at conventional MR, because changes in tumor physiology may precede structural changes.

DSC MR perfusion can be performed on any modern MR scanner, has a short acquisition time, and postprocessing software is widely available.<sup>33</sup> However, it has some inherent limitations. Blood products or melanin within brain metastases can cause a significant degree of susceptibility artifacts, impeding assessment.<sup>11,23</sup>

Furthermore, metastases may not be evaluable if they are too small or near large vessels or bone.<sup>23</sup> In this systematic review, the median percentage of uninterpretable lesions was 5.35%.

The studies that measured rCBV showed variation in region of interest (ROI) placement: ROIs were placed encompassing the entire contrast-enhancing lesion<sup>21,22,26</sup> or in selected areas of the contrast-enhancing lesion,<sup>8,11,20,29</sup> whereas in some studies the method of ROI placement was not described.<sup>28,30</sup> Some studies measured mean values, whereas other studies measured maximum values. The mean value varies depending on which voxels are included in the average, making it sensitive to ROI definition. The maximum value is less dependent on ROI definition (assuming the voxel with highest CBV and no normal macrovessels are included) but more susceptible to noise. Only two of the included studies reported interobserver reproducibility.<sup>20,22</sup> Wang et al<sup>20</sup> reported good interobserver agreement for mean rCBV. Muto et al<sup>22</sup> also reported good interobserver agreement, but did not specify whether this applied to mean or maximum rCBV. Furthermore, it has recently been shown that ROI placement in the semioval center as reference tissue provides the highest interobserver agreement.<sup>34</sup> However, only one of the included studies reported using the semioval center as reference tissue.<sup>30</sup> One other study used the normal-appearing contralateral white matter (NACWM) on the same transaxial plane as the lesion as reference tissue,<sup>11</sup> whereas in the other studies<sup>8,20–22,26,28,29</sup> the exact location of ROI placement in the NACWM was not reported.

Exploratory subgroup analyses suggested that publication year, country of origin, study size, and DSC MR perfusion interpretation methods were no causes of heterogeneity. ROC curve analysis of the only included study that performed both visual analysis of CBV map and rCBV measurement<sup>30</sup> also showed that diagnostic accuracy between both perfusion interpretation methods was not significantly different. Pretreatment rCBV of brain metastases from renal carcinoma and melanoma are significantly higher than rCBV of brain metastases from lung, breast, and gastrointestinal carcinoma.<sup>35,36</sup> Furthermore, it has been shown by microscopy that neovascularization patterns of brain

**TABLE 3. Subgroup Analyses**

Parameter	Variables <sup>a</sup>	Relative diagnostic odds ratio <sup>b</sup>	P value
Publication year	Published after (5) vs. published before 2013 (5)	2.21 (0.14, 34.01)	0.5157
Country of origin	USA (6) vs. Other countries (4)	0.21 (0.01, 2.92)	0.2030
Study size	>28 patients (5) vs. <28 (5)	1.88 (0.11, 31.20)	0.6101
DSC MR perfusion interpretation method	Visual analysis of CBV map (2) vs. measurement of rCBV (7)	0.22 (0.01, 8.93)	0.3554

<sup>a</sup>Data in parentheses are number of studies.  
<sup>b</sup>Data in parentheses are 95% CIs.

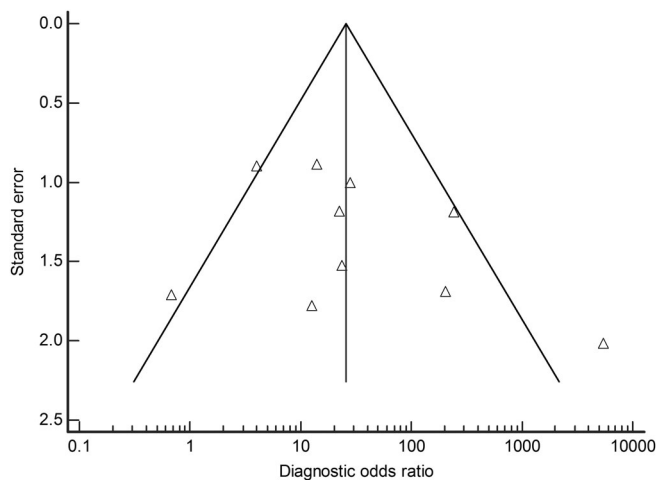


**FIGURE 7: Funnel plot using the diagnostic odds ratio of the 10 included studies. \*Two diagonal lines represent 95% confidence limits (effect  $\pm 1.96$  standard error) around the summary effect (vertical line) for each standard error on the vertical axis.**

metastases from a different origin can be quite different. For instance, neovascularization is a specific hallmark of nonsmall-cell lung cancer metastases, whereas melanoma metastases show less neovascularization and more perivascular growth along pre-existing vascular structures.<sup>37</sup> Therefore, one may expect that the diagnostic performance of DSC MR perfusion differs considerably among different tumor entities. However, all included studies pooled metastases of different primary tumor origin together, so it was not possible to investigate the influence of primary tumor origin on accuracy. Another potential source of heterogeneity is the use of different definitions for recurrent metastases in studies using histopathology as the reference standard. Other potential sources of heterogeneity are variations in MR parameters (such as the use of preload, leakage correction, injection rate, flip angle, and temporal coverage), postprocessing methods (for leakage correction), and diagnostic criteria. Unfortunately, due to large variability between studies, we could not perform meaningful subgroup analyses for these parameters.

This systematic review has some limitations. First, the number of included studies was relatively low. Therefore, we could not fully explore potential sources of heterogeneity with subgroup analysis or meta-regression. Second, the funnel plot which suggested the absence of publication bias is not always a reliable tool.<sup>38,39</sup>

Conventional MRI findings of treatment-related changes and metastatic recurrence overlap considerably.<sup>4-6</sup> Therefore, DSC MR perfusion can be a very useful adjunct in diagnosing recurrent brain metastases after radiotherapy. However, pooled sensitivity and specificity of DSC MR perfusion were fairly high, but not perfect. Furthermore, it is still questionable whether these pooled overall results can be applied to all metastases of different primary origin and there is no uniformly accepted diagnostic criterion yet. Therefore, one should be careful to make clinical decisions based on DSC MR perfusion results alone. The question remains as to what represents "best practice" based on

current evidence. We suggest that DSC MR perfusion acquisitions are performed according to recommendations from the American Society of Functional Neuroradiology (ASFNR).<sup>12</sup> According to the ASFNR, preload administration of a single contrast agent bolus with postprocessing leakage correction and implicit correction of  $T_1$  leakage effects with a dual-echo acquisition methodology are the two methods that best distinguish rCBV in tumor from normal brain in the presence of contrast agent leakage effects.<sup>12</sup> We suggest that either one of these methods is used. We found no evidence that either visual analysis of CBV maps or rCBV measurements performed better than the other in terms of diagnostic accuracy. Therefore, at present it may be justified to use either one of these perfusion interpretation methods. We believe that all MRI results should be interpreted in the clinical context (including patient symptoms and clinical findings, date and type of treatment received, and systemic status). This is preferably discussed in a neuro-oncology multidisciplinary team meeting, which is the optimal place to make decisions regarding further diagnostic work-up (such as closer follow-up or stereotactic biopsy) and treatment.<sup>40,41</sup>

In order to validate DSC MR perfusion for clinical application, it is essential to further investigate potential causes of heterogeneity. Ideally, this is done by prospective studies following ASFNR recommendations regarding DSC MR perfusion acquisition and postprocessing. Future studies should make a direct comparison between DSC MR perfusion interpretation methods and perform stratified analysis for metastases per primary tumor type. Diagnostic accuracy may be improved by combining DSC MR perfusion with other advanced MR techniques<sup>25</sup> or positron emission tomography,<sup>42,43</sup> but this also needs further investigation.

In conclusion, the results of our study suggest that the accuracy of DSC MR perfusion in diagnosing recurrent brain metastases after radiotherapy is fairly high. However, these findings should be interpreted with caution because of methodological quality concerns and heterogeneity between studies. There is no uniformly accepted diagnostic criterion to define metastatic recurrence yet. Potential causes of heterogeneity need to be further investigated.

## References

1. Lin X, DeAngelis LM. Treatment of brain metastases. *J Clin Oncol* 2015;33:3475-3484.
2. Cagney DN, Martin AM, Catalano PJ, et al. Incidence and prognosis of patients with brain metastases at diagnosis of systemic malignancy: A population-based study. *Neuro Oncol* 2017;19:1511-1521.
3. Patel TR, McHugh BJ, Bi WL, Minja FJ, Knisely JP, Chiang VL. A comprehensive review of MR imaging changes following radiosurgery to 500 brain metastases. *AJNR Am J Neuroradiol* 2011;32:1885-1892.
4. Shah R, Vattoth S, Jacob R, et al. Radiation necrosis in the brain: Imaging features and differentiation from tumor recurrence. *Radiographics* 2012;32:1343-1359.
5. Stockham AL, Tievsky AL, Koyfman SA, et al. Conventional MRI does not reliably distinguish radiation necrosis from tumor recurrence after stereotactic radiosurgery. *J Neurooncol* 2012;109:149-158.

6. Dooms GC, Hecht S, Brant-Zawadzki M, Berthiaume Y, Norman D, Newton TH. Brain radiation lesions: MR imaging. *Radiology* 1986;158:149–155.
7. Dequesada IM, Quisling RG, Yachnis A, Friedman WA. Can standard magnetic resonance imaging reliably distinguish recurrent tumor from radiation necrosis after radiosurgery for brain metastases? A radiographic-pathological study. *Neurosurgery* 2008 Nov;63:898–903.
8. Truong MT, St Clair EG, Donahue BR, et al. Results of surgical resection for progression of brain metastases previously treated by gamma knife radiosurgery. *Neurosurgery* 2006;59:86–97.
9. Koiso T, Yamamoto M, Kawabe T, et al. Follow-up results of brain metastasis patients undergoing repeat gamma knife radiosurgery. *J Neurosurg* 2016;125(Suppl 1):2–10.
10. Malone H, Yang J, Hershman DL, Wright JD, Bruce JN, Neugut AI. Complications following stereotactic needle biopsy of intracranial tumors. *World Neurosurg* 2015;84:1084–1089.
11. Barajas RF, Chang JS, Sneed PK, Segal MR, McDermott MW, Cha S. Distinguishing recurrent intra-axial metastatic tumor from radiation necrosis following gamma knife radiosurgery using dynamic susceptibility-weighted contrast-enhanced perfusion MR imaging. *AJNR Am J Neuroradiol* 2009;30:367–372.
12. Welker K, Boxerman J, Kalnin A, Kaufmann T, Shiroishi M, Wintermark M; American Society of Functional Neuroradiology MR Perfusion Standards and Practice Subcommittee of the ASFN Clinical Practice Committee. ASFN recommendations for clinical performance of MR dynamic susceptibility contrast perfusion imaging of the brain. *AJNR Am J Neuroradiol* 2015;36:E41–51.
13. Whiting PF, Rutjes AW, Westwood ME, et al. QUADAS-2 Group. QUADAS-2: A revised tool for the quality assessment of diagnostic accuracy studies. *Ann Intern Med* 2011;155:529–536.
14. Reitsma JB, Glas AS, Rutjes AW, Scholten RJ, Bossuyt PM, Zwinderman AH. Bivariate analysis of sensitivity and specificity produces informative summary measures in diagnostic reviews. *J Clin Epidemiol* 2005;58:982–990.
15. Glas AS, Lijmer JG, Prins MH, Bonsel GJ, Bossuyt PM. The diagnostic odds ratio: A single indicator of test performance. *J Clin Epidemiol* 2003;56:1129–1135.
16. DeLong ER, DeLong DM, Clarke-Pearson DL. Comparing the areas under two or more correlated receiver operating characteristic curves: A nonparametric approach. *Biometrics* 1988;44:837–845.
17. Egger M, Davey Smith G, Schneider M, Minder C. Bias in meta-analysis detected by a simple, graphical test. *BMJ* 1997;315:629–634.
18. <https://www.r-project.org/>
19. <https://www.rdocumentation.org/packages/mada/versions/0.5.8/topics/mada-package>
20. Wang B, Zhao B, Zhang Y, et al. Absolute CBV for the differentiation of recurrence and radionecrosis of brain metastases after gamma knife radiotherapy: A comparison with relative CBV. *Clin Radiol* 2018;73:758.e1–758.e7.
21. Knitter JR, Erly WK, Stea BD, et al. Interval change in diffusion and perfusion MRI parameters for the assessment of pseudoprogression in cerebral metastases treated with stereotactic radiation. *AJR Am J Roentgenol* 2018;211:168–175.
22. Muto M, Frauenfelder G, Senese R, et al. Dynamic susceptibility contrast (DSC) perfusion MRI in differential diagnosis between radionecrosis and neoangiogenesis in cerebral metastases using rCBV, rCBF and K<sub>2</sub>. *Radiol Med* 2018;123:545–552.
23. Kerkhof M, Ganef I, Wiggenraad RGJ, et al. Clinical applicability of and changes in perfusion MR imaging in brain metastases after stereotactic radiotherapy. *J Neurooncol* 2018;138:133–139.
24. Jakubovic R, Sahgal A, Ruschin M, Pejović-Milić A, Milwid R, Aviv RI. Non tumor perfusion changes following stereotactic radiosurgery to brain metastases. *Technol Cancer Res Treat* 2015;14:497–503.
25. Koh MJ, Kim HS, Choi CG, Kim SJ. Which is the best advanced MR imaging protocol for predicting recurrent metastatic brain tumor following gamma-knife radiosurgery: Focused on perfusion method. *Neuroradiology* 2015;57:367–376.
26. Cicone F, Minniti G, Romano A, et al. Accuracy of F-DOPA PET and perfusion-MRI for differentiating radionecrotic from progressive brain metastases after radiosurgery. *Eur J Nucl Med Mol Imaging* 2015;42:103–111.
27. Jakubovic R, Sahgal A, Soliman H, et al. Magnetic resonance imaging-based tumour perfusion parameters are biomarkers predicting response after radiation to brain metastases. *Clin Oncol (R Coll Radiol)* 2014;26:704–712.
28. Huang J, Wang AM, Shetty A, et al. Differentiation between intra-axial metastatic tumor progression and radiation injury following fractionated radiation therapy or stereotactic radiosurgery using MR spectroscopy, perfusion MR imaging or volume progression modeling. *Magn Reson Imaging* 2011;29:993–1001.
29. Mitsuya K, Nakasu Y, Horiguchi S, et al. Perfusion weighted magnetic resonance imaging to distinguish the recurrence of metastatic brain tumors from radiation necrosis after stereotactic radiosurgery. *J Neurooncol* 2010;99:81–88.
30. Hoefnagels FW, Lagerwaard FJ, Sanchez E, et al. Radiological progression of cerebral metastases after radiosurgery: Assessment of perfusion MRI for differentiating between necrosis and recurrence. *J Neurol* 2009;256:878–887.
31. Weber MA, Thilman C, Lichy MP, et al. Assessment of irradiated brain metastases by means of arterial spin-labeling and dynamic susceptibility-weighted contrast-enhanced perfusion MRI: Initial results. *Invest Radiol* 2004;39:277–287.
32. Essig M, Waschkies M, Wenz F, Debus J, Hentrich HR, Knopp MV. Assessment of brain metastases with dynamic susceptibility-weighted contrast-enhanced MR imaging: Initial results. *Radiology* 2003;228:193–199.
33. Essig M, Shiroishi MS, Nguyen TB, et al. Perfusion MRI: The five most frequently asked technical questions. *AJR Am J Roentgenol* 2013;200:24–34.
34. Oei MTH, Meijer FJA, Mordang JJ, et al. Observer variability of reference tissue selection for relative cerebral blood volume measurements in glioma patients. *Eur Radiol* 2018;28:3902–3911.
35. Zhang H, Zhang G, Oudkerk M. Brain metastases from different primary carcinomas: An evaluation of DSC MRI measurements. *Neuroradiol J* 2012;25:67–75.
36. Kremer S, Grand S, Berger F, et al. Dynamic contrast-enhanced MRI: Differentiating melanoma and renal carcinoma metastases from high-grade astrocytomas and other metastases. *Neuroradiology* 2003;45:44–49.
37. Kienast Y, von Baumgarten L, Fuhrmann M, et al. Real-time imaging reveals the single steps of brain metastasis formation. *Nat Med* 2010;16:116–122.
38. Lau J, Ioannidis JP, Terrin N, Schmid CH, Olkin I. The case of the misleading funnel plot. *BMJ* 2006;333:597–600.
39. Biljana M, Jelena M, Branislav J, Milorad R. Bias in meta-analysis and funnel plot asymmetry. *Stud Health Technol Inform* 1999;68:323–328.
40. Ameratunga M, Miller D, Ng W, et al. A single-institution prospective evaluation of a neuro-oncology multidisciplinary team meeting. *J Clin Neurosci* 2018;56:127–130.
41. Loh D, Hogg F, Edwards P, et al. Two-year experience of multidisciplinary team (MDT) outcomes for brain metastases in a tertiary neuro-oncology centre. *Br J Neurosurg* 2018;32:53–60.
42. Fink JR, Muzi M, Peck M, Krohn KA. Multimodality brain tumor imaging: MR Imaging, PET, and PET/MR Imaging. *J Nucl Med* 2015;56:1554–1561.
43. Li H, Deng L, Bai HX, et al. Diagnostic accuracy of amino acid and FDG-PET in differentiating brain metastasis recurrence from radionecrosis after radiotherapy: A systematic review and meta-analysis. *AJNR Am J Neuroradiol* 2018;39:280–288.